

Crystal Structures and Hydrogen Bonding in One-Dimensional Chains of 4,5-Dicyanoimidazole and 4,5-Dichloroimidazole

Shigenori Nagatomo, Sadamu Takeda,* Hatsue Tamura,† and Nobuo Nakamura

Department of Chemistry, Faculty of Science, Osaka University, Toyonaka, Osaka 560

†Department of Applied Chemistry, Faculty of Engineering, Osaka University, Toyonaka, Osaka 560

(Received December 15, 1994)

The crystal structure of 4,5-dicyanoimidazole ((CN)₂Imd) was determined by an X-ray diffraction at room temperature; monoclinic, $P2_1/a$, $a=7.259(2)$, $b=7.529(1)$, $c=10.0972(9)$ Å, $\beta=102.74(1)^\circ$, $V=538.2(2)$ Å³, $Z=4$, $R=0.043$, and $R_w=0.066$ for 1090 observed reflections. Crystal structure of 4,5-dichloroimidazole (Cl₂Imd) was redetermined; tetragonal, $P4_12_12$, $a=6.843(4)$, $c=24.236(7)$ Å, $V=1134(1)$ Å³, $Z=8$, $R=0.043$, and $R_w=0.058$ for 427 observed reflections. Molecules in Cl₂Imd and in (CN)₂Imd are linked by intermolecular N–H···N hydrogen bonds to form one-dimensional chains. The hydrogen bonds in Cl₂Imd are formed between the ring nitrogen atoms, while those in (CN)₂Imd are between the ring and the cyano nitrogens. The hydrogen bond distance (3.051(2) Å) of N···N in (CN)₂Imd is long, compared with that (2.800(6) Å) in Cl₂Imd. The weak hydrogen bond in (CN)₂Imd was also indicated by IR and ¹⁵N CP/MAS NMR spectra.

In the crystals of imidazole^{1–4)} and 4-nitroimidazole,^{5,6)} successive intermolecular N–H···N hydrogen bonds are formed between the ring nitrogens in adjacent molecules to construct one-dimensional chains. Early measurements of second moment of proton NMR⁷⁾ and of conductivity⁸⁾ suggested that the proton motion occurs in the solid state of imidazole. On the other hand, X-ray and neutron diffraction studies of imidazole at room temperature and 123 K indicated that the hydrogen atom in the hydrogen bond is almost localized at one of the nitrogen atoms.^{3,4)} It is thus interesting to investigate the possibility and mechanism of the proton motion within the hydrogen bond, as well as long-range proton transfer in the one-dimensional chain in imidazole and its derivatives.

In the course of series of NMR studies of proton dynamics in one-dimensional hydrogen bonded chain systems, we examined the crystal structures of 4,5-dicyanoimidazole ((CN)₂Imd) and 4,5-dichloroimidazole (Cl₂Imd). The crystal structure of Cl₂Imd has been determined by Dou and Weiss.⁹⁾ The equivalent reflections seem to have been included in their structure determination, because the number of independent reflections collected up to $\sin \theta/\lambda=0.005385$ pm^{–1} is not 744 but about 525. They reported that two non-equivalent C–Cl bond lengths in a molecule coincide accidentally with each other. Two non-equivalent C–N bond lengths in the ring are also reported to be very similar compared with the case of imidazole.^{1–4)} This point seems important in relation to the possible proton motion in

the intermolecular N–H···N hydrogen bond. We therefore tried to redetermine the more precise structure of Cl₂Imd by an X-ray diffraction method. Infrared (IR) and the natural abundance ¹⁵N CP/MAS (cross polarization/magic angle spinning) NMR spectra were also measured to characterize the hydrogen bonds in Cl₂Imd and (CN)₂Imd.

Experimental

1. Materials. The compound Cl₂Imd was purchased from Tokyo Kasei Kogyo Co., Ltd. and (CN)₂Imd was from Aldrich Chemical Company, Inc. Colorless prismatic crystals of Cl₂Imd and (CN)₂Imd for the X-ray diffraction experiments were obtained by slow evaporation of aqueous solution and of diethyl ether solution at room temperature, respectively. In the case of the compound (CN)₂Imd, other crystals of the monohydrate, C₅H₂N₄·H₂O, were obtained from the equimolar solution of acetone and water. The crystals were easily dehydrated in vacuo at room temperature or on heating up to ca. 50 °C under the atmosphere; the dried powder sample thus obtained gave exactly the same powder diffraction pattern as the crystals (CN)₂Imd grown from diethyl ether solution.

2. Measurements. The specimens dried in vacuo (10^{–3} mmHg, 1 mmHg=133.322 Pa) were used for IR and NMR measurements. The IR spectra of the specimens dispersed in KBr disks, dried Nujol, and Fluorinert (FC40) were recorded on a JASCO FT/IR-3 and a JASCO FT/IR-8300 at room temperature. They were identical with each other in the whole frequency region except in the blind one of Nujol and FC40. This indicates the dispersion media do not affect the specimens. FC40 is transparent for IR above 1400

cm^{-1} . The natural abundance ^{15}N CP/MAS NMR spectrum at room temperature was measured by Bruker MSL200 and DSX300 spectrometers at the resonance frequencies of 20.3 and 30.4 MHz with the contact time between 1 and 4 ms and the field strength of ca. 30 kHz for proton decoupling. Repetition time was between 100 and 600 s and the number of accumulations was between 140 and 750. The chemical shifts were measured relative to ^{15}N of nitromethane; powdered glycine labeled by ^{15}N was used as an external reference (-347.5 ppm^{10}).

3. Crystal Structure Determination. Crystal data, the details of the data collection and the structure refinement of Cl_2Imd and $(\text{CN})_2\text{Imd}$ are listed in Table 1. Intensity data were collected at room temperature using a Rigaku AFC-5R diffractometer with graphite monochromated $\text{Mo } K\alpha$ radiation at the X-ray Diffraction Service of

the Department of Chemistry, Faculty of Science, Osaka University.

The systematic absences $h00: h \neq 2n$, $00l: l \neq 4n$ indicated the possible space groups $P4_12_12$ and $P4_32_12$ for Cl_2Imd . Since it was difficult to distinguish clearly between $P4_12_12$ and $P4_32_12$ by the absolute configuration analysis and the comparison of their R values, the space group of Cl_2Imd was made to be $P4_12_12$, which is identical to the reported space group.⁹ The systematic absences $h0l: h \neq 2n$, $0k0: k \neq 2n$ showed uniquely the space group of $P2_1/a$ for $(\text{CN})_2\text{Imd}$. The structures were solved by the direct methods using SHELXS86¹¹ and SAPI91.¹² The function $\sum w(|F_o| - |F_c|)^2$ with $w = (\sigma^2(F_o) + 0.0009F_o^2)^{-1}$ was minimized for the refinement. All hydrogen atoms were located from difference Fourier maps (DIRDIF92¹³). The thermal parameters were refined anisotropically for non-hydrogen atoms and

Table 1. Crystal Data, Details of Data Collection and Structure Refinement

	Cl_2Imd	$(\text{CN})_2\text{Imd}$
Color	Colorless	Colorless
Crystal shape	Prisms	Prisms
Molecular formula	$\text{C}_3\text{H}_2\text{N}_2\text{Cl}_2$	$\text{C}_5\text{H}_2\text{N}_4$
Formula weight	136.97	118.10
Crystal size/mm	$0.3 \times 0.2 \times 0.7$	$0.3 \times 0.3 \times 0.4$
Crystal system	Tetragonal	Monoclinic
Space group	$P4_12_12$	$P2_1/a$
$a/\text{\AA}$	6.843(4)	7.259(2)
$b/\text{\AA}$		7.529(1)
$c/\text{\AA}$	24.236(7)	10.0972(9)
$\beta/^\circ$		102.74(1)
$V/\text{\AA}^3$	1134(1)	538.2(2)
Z	8	4
$D_c/\text{Mg m}^{-3}$	1.603	1.457
Radiation	$\text{Mo } K\alpha$	$\text{Mo } K\alpha$
$\lambda/\text{\AA}$	0.71069	0.71069
μ/mm^{-1}	1.007	0.102
For cell parameter		
$2\theta/^\circ$	20.2—25.0	29.0—29.9
No. of reflections	25	25
Scan range $2\theta/^\circ$	60.0	60.1
Scan width $\Delta\omega/^\circ$	$1.85 + 0.30 \tan \theta$	$1.78 + 0.35 \tan \theta$
Scan speed ω/min^{-1}	16	4
Scan mode	ω	$2\theta - \omega$
Monitored reflections (every 100 reflections)	$\bar{1}\bar{1}\bar{6}$ $\bar{1}\bar{1}\bar{6}$ $2\bar{1}\bar{1}$	$20\bar{1}$ $00\bar{2}$ $\bar{1}\bar{1}\bar{2}$
Variation of intensities	0.019	0.024
Range of h, k, l	0—10, 0—10, 0—34	0—10, 0—11, -14—14
Transmission factor		
$A_{\min} - A_{\max}$	0.84—1.00	0.97—1.00
No. of reflections		
Measured	1967	1821
Unique	1083	1704
Observed ($ I > 3\sigma(I)$)	427	1090
R_{int}	0.046	0.016
R	0.043	0.043
R_w	0.058	0.066
$\Delta\rho_{\min} - \Delta\rho_{\max}/e \text{\AA}^{-3}$	-0.21—+0.27	-0.23—+0.24
$(\Delta/\sigma)_{\max}$	0.04	0.10
S	1.43	1.61

Table 2. Atomic Coordinates and Equivalent Isotropic Thermal Parameters (\AA^2) with Their esd's in Parentheses for Cl_2Imd ; $B_{\text{eq}} = \frac{8\pi^2}{3} (U_{11} + U_{22} + U_{33})$

Atoms	<i>x</i>	<i>y</i>	<i>z</i>	$B_{\text{eq}}/B_{\text{iso}}$
N(1)	0.3814(8)	-0.0668(7)	0.9861(2)	5.5(1)
C(2)	0.3228(10)	-0.2387(10)	1.0054(3)	6.5(2)
N(3)	0.1563(8)	-0.2941(8)	0.9826(2)	6.1(1)
C(4)	0.1128(8)	-0.1504(8)	0.9464(2)	4.8(1)
C(5)	0.2503(9)	-0.0112(8)	0.9481(2)	4.9(1)
Cl(4)	-0.0888(3)	-0.1607(3)	0.90543(8)	8.74(6)
Cl(5)	0.2732(3)	0.2024(3)	0.91270(7)	8.16(5)
H(1)	0.48(1)	-0.02(1)	0.998(3)	9.3(9)
H(2)	0.39(1)	-0.30(1)	1.036(2)	7.4(10)

Anisotropic Displacement Parameters (\AA^2) with Their esd's in Parentheses for Cl_2Imd ;
 The General Temperature Factor Expression:
 $\exp(-2\pi^2(a^{*2}U_{11}h^2 + b^{*2}U_{22}k^2 + c^{*2}U_{33}l^2 + 2a^*b^*U_{12}hk + 2a^*c^*U_{13}hl + 2b^*c^*U_{23}kl))$

Atom	U_{11}	U_{22}	U_{33}	U_{12}	U_{13}	U_{23}
N(1)	0.067(3)	0.068(3)	0.075(3)	-0.033(3)	-0.003(3)	-0.001(2)
C(2)	0.094(5)	0.076(5)	0.078(4)	-0.037(4)	-0.012(4)	0.013(4)
N(3)	0.075(3)	0.071(3)	0.085(3)	-0.041(3)	-0.004(3)	0.004(3)
C(4)	0.054(3)	0.062(3)	0.065(3)	-0.013(3)	0.000(3)	-0.013(3)
C(5)	0.067(4)	0.056(3)	0.063(3)	-0.018(3)	0.004(3)	-0.006(3)
Cl(4)	0.082(1)	0.107(2)	0.143(2)	-0.019(1)	-0.040(1)	-0.012(1)
Cl(5)	0.116(2)	0.073(1)	0.121(1)	-0.025(1)	-0.003(1)	0.024(1)

isotropically for hydrogen atoms. All calculations were performed using crystallographic software package *teXsan*¹⁴⁾ on an IRIS INDIGO workstation at Faculty of Science, Osaka University.

The final positional and thermal parameters for Cl_2Imd and $(\text{CN})_2\text{Imd}$ are listed in Tables 2 and 4, respectively. ORTEP¹⁵⁾ views with the numbering scheme are given in Fig. 1 for Cl_2Imd and Fig. 3 for $(\text{CN})_2\text{Imd}$. Tables 3 and 5 show the bond distances and the bond angles for Cl_2Imd and $(\text{CN})_2\text{Imd}$, respectively. Complete lists of the structure factors for Cl_2Imd and $(\text{CN})_2\text{Imd}$ were deposited as Document No. 68055 at the Office of the Editor of Bull. Chem. Soc. Jpn.

Table 3. Bond Distances, Angles, and Hydrogen Bond Distances, Angle in Cl_2Imd

Bond distances (\AA)		Bond angles (deg.)	
N(1)-C(2)	1.328(7)	N(1)-C(2)-N(3)	111.5(5)
C(2)-N(3)	1.323(7)	C(2)-N(3)-C(4)	104.7(4)
N(3)-C(4)	1.350(7)	N(3)-C(4)-C(5)	110.1(5)
C(4)-C(5)	1.339(7)	C(4)-C(5)-N(1)	106.8(5)
C(5)-N(1)	1.341(7)	C(5)-N(1)-C(2)	107.0(5)
C(4)-Cl(4)	1.701(6)	Cl(4)-C(4)-N(3)	121.8(4)
C(5)-Cl(5)	1.702(6)	Cl(4)-C(4)-C(5)	128.1(5)
		Cl(5)-C(5)-N(1)	121.9(4)
		Cl(5)-C(5)-C(4)	131.3(5)
N(1)-H(1)	0.82(8)	C(5)-N(1)-H(1)	133(6)
C(2)-H(2)	0.98(6)	C(2)-N(1)-H(1)	120(6)
		N(1)-C(2)-H(2)	120(4)
		N(3)-C(3)-H(2)	128(4)
Hydrogen bond distances (\AA)		Hydrogen bond angle (deg.)	
H(1)⋯N(3)	2.00(8)	N(1)-H(1)⋯N(3)	167(9)
N(1)⋯N(3)	2.800(6)		

Results and Discussion

1. Structure and Spectroscopic Properties of Cl_2Imd .

As shown in Fig. 2, the crystal structure of Cl_2Imd consists of one-dimensional chains of the molecules linked by intermolecular N-H⋯N hydrogen bonds between ring nitrogen atoms as in the case of imidazole¹⁻⁴⁾ and 4-nitroimidazole.^{5,6)} The one-dimensional hydrogen-bonded chains run in two different directions, [110] and $[\bar{1}10]$, which are related to each other by the fourfold screw axis parallel to the *c* axis. The arrangement of the hydrogen-bonded chains is quite different from those in imidazole and 4-nitroimidazole in which the chains run only in one direction. The intermolecular hydrogen bond distance (2.800(6) \AA) of N⋯N is shorter than those in imidazole (2.86 \AA at 123 K⁴⁾) and 4-nitroimidazole (2.871(3) \AA at 293 K⁵⁾) and 2.864(2) \AA at 100 K⁶⁾), and the angle (167(9)°) of N-H⋯N is similar to those of the related compounds (174° at 123 K⁴⁾ in imidazole, 167(3)° at 293 K⁵⁾ and 174.2(1)° at 100 K⁶⁾ in 4-nitroimidazole).

The strong hydrogen bond in Cl_2Imd was also supported by the relatively large low-frequency shift of N-H stretching mode (ν_{NH}),¹⁶⁾ as shown in Fig. 5(a). The stretching modes of N-H and N-D are assigned to be 2570 and 2080 cm^{-1} , respectively (Fig. 5(a) and (b')). The C-H proton was also deuterated because the C-H stretching mode ($\nu_{\text{CH}}=3140 \text{ cm}^{-1}$), which was observed by IR and Raman, did not appear in the deuterated compound (Fig. 5(b')). The ratio between the frequencies at maxima of broad absorption bands, $\nu_{\text{NH}}/\nu_{\text{ND}}=1.2$, is smaller than $\sqrt{2}$, suggesting that the anharmonic-

Table 4. Atomic Coordinates and Equivalent Isotropic Thermal Parameters (\AA^2) with Their esd's in Parentheses for $(\text{CN})_2\text{Imd}$; $B_{\text{eq}} = \frac{8\pi^2}{3} (U_{11} + U_{22} + U_{33} + 2U_{13}\cos\beta)$

Atoms	<i>x</i>	<i>y</i>	<i>z</i>	$B_{\text{eq}}/B_{\text{iso}}$
N(1)	0.5126(2)	0.2967(2)	0.7506(1)	2.70(3)
C(2)	0.3995(3)	0.2807(2)	0.6261(2)	2.92(3)
N(3)	0.3648(2)	0.1140(2)	0.5894(1)	3.12(3)
C(4)	0.4628(2)	0.0182(2)	0.6967(1)	2.66(3)
C(5)	0.5556(2)	0.1285(2)	0.7979(1)	2.48(3)
C(41)	0.4634(3)	-0.1703(2)	0.7013(2)	3.68(4)
N(42)	0.4658(3)	-0.3210(2)	0.7087(2)	5.76(5)
C(51)	0.6730(2)	0.0822(2)	0.9251(2)	3.07(3)
N(52)	0.7649(2)	0.0324(2)	1.0242(2)	4.50(4)
H(1)	0.552(3)	0.408(3)	0.794(2)	4.9(5)
H(2)	0.348(3)	0.381(3)	0.575(2)	3.0(4)

Anisotropic Displacement Parameters (\AA^2) with Their esd's in Parentheses for $(\text{CN})_2\text{Imd}$;
The General Temperature Factor Expression:

$$\exp(-2\pi^2(a^{*2}U_{11}h^2 + b^{*2}U_{22}k^2 + c^{*2}U_{33}l^2 + 2a^*b^*U_{12}hk + 2a^*c^*U_{13}hl + 2b^*c^*U_{23}kl))$$

Atom	U_{11}	U_{22}	U_{33}	U_{12}	U_{13}	U_{23}
N(1)	0.0446(8)	0.0212(6)	0.0332(7)	-0.0009(5)	0.0011(5)	-0.0003(5)
C(2)	0.0476(9)	0.0259(8)	0.0335(7)	0.0037(6)	0.0006(6)	0.0031(6)
N(3)	0.0520(8)	0.0273(7)	0.0324(7)	0.0032(6)	-0.0057(6)	0.0001(5)
C(4)	0.0436(8)	0.0227(6)	0.0299(7)	0.0011(6)	-0.0027(6)	-0.0004(5)
C(5)	0.0385(8)	0.0238(7)	0.0293(7)	-0.0013(6)	0.0016(6)	0.0010(5)
C(41)	0.0612(11)	0.0257(8)	0.0421(9)	-0.0008(7)	-0.0117(8)	-0.0007(7)
N(42)	0.1026(16)	0.0259(8)	0.0705(12)	0.0012(8)	-0.0234(11)	0.0003(8)
C(51)	0.0458(9)	0.0319(8)	0.0337(8)	-0.0039(7)	-0.0024(6)	-0.0001(6)
N(52)	0.0663(11)	0.0517(10)	0.0420(8)	-0.0002(9)	-0.0121(7)	0.0068(7)

Table 5. Bond Distances, Angles, and Hydrogen Bond Distances, Angles in $(\text{CN})_2\text{Imd}$

Bond distances (\AA)		Bond angles (deg.)	
N(1)-C(2)	1.346(2)	N(1)-C(2)-N(3)	112.8(1)
C(2)-N(3)	1.317(2)	C(2)-N(3)-C(4)	104.2(1)
N(3)-C(4)	1.365(2)	N(3)-C(4)-C(5)	110.8(1)
C(4)-C(5)	1.373(2)	C(4)-C(5)-N(1)	105.3(1)
C(5)-N(1)	1.364(2)	C(5)-N(1)-C(2)	106.8(1)
C(4)-C(41)	1.420(2)	N(3)-C(4)-C(41)	123.5(1)
C(41)-N(42)	1.137(2)	C(5)-C(4)-C(41)	125.7(1)
C(5)-C(51)	1.420(2)	C(4)-C(41)-N(42)	178.1(2)
C(51)-N(52)	1.137(2)	C(4)-C(5)-C(51)	128.5(1)
		N(1)-C(5)-C(51)	126.2(1)
		C(5)-C(51)-N(52)	175.0(2)
N(1)-H(1)	0.96(3)	C(2)-N(1)-H(1)	124(1)
C(2)-H(2)	0.94(2)	C(5)-N(1)-H(1)	129(1)
		N(1)-C(2)-H(2)	122(1)
		N(3)-C(2)-H(2)	125(1)
Hydrogen bond distances (\AA)		Hydrogen bond angles (deg.)	
H(1)...N(52)	2.22(2)	N(1)-H(1)...N(52)	144(2)
H(1)...N(42)	2.25(3)	N(1)-H(1)...N(42)	126(2)
N(1)...N(52)	3.051(2)		
N(1)...N(42)	2.918(2)		

ity of this N-H stretching mode is due probably to the extremely asymmetric potential energy function for H in the N(1)-H...N(3') hydrogen bond. The apparent maximum value of the electron density for the proton-transferred configuration (N(1)...H-N(3')) was not detected

by X-ray diffraction. In the measurement of the natural abundance ^{15}N CP/MAS NMR spectrum on the powdered sample, two signals were observed; -200.0 and -133.3 ppm for $>\text{N}(1)-$ and $=\text{N}(3)-$, respectively. The difference between the chemical shifts of the two nitro-

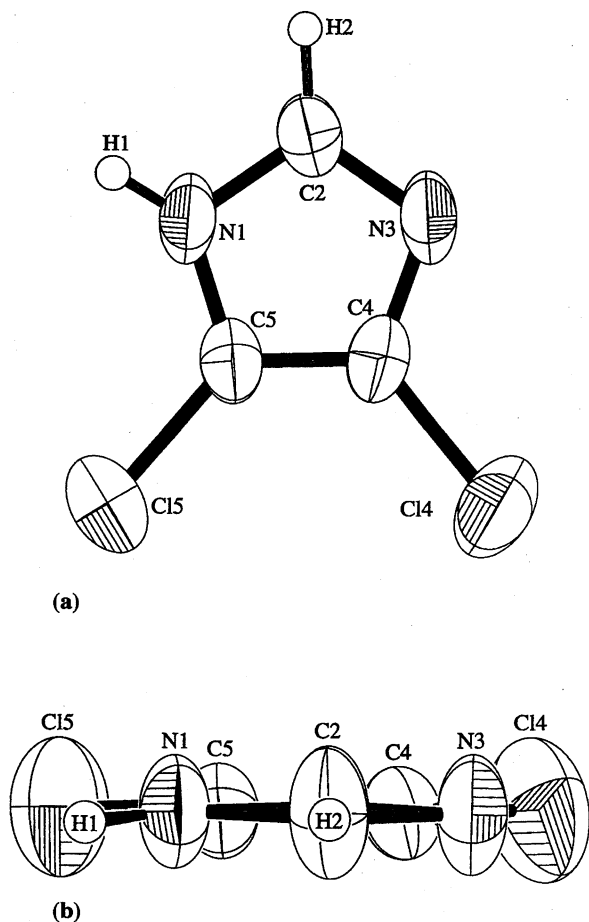


Fig. 1. ORTEP views of 4,5-dichloroimidazole with a numbering scheme; viewed along a direction perpendicular to the plane of the ring (a) and parallel to one (b). Thermal ellipsoids are shown at 40% probability level.

gen nuclei in Cl_2Imd is smaller than that in $(\text{CN})_2\text{Imd}$, as described in the next section. The similar tendency is also seen in the difference of the bond lengths between $\text{C}(2)-\text{N}(1)$ and $\text{C}(2)-\text{N}(3)$: the differences of them are 0.005(10) and 0.029(3) Å for Cl_2Imd and $(\text{CN})_2\text{Imd}$, respectively.

Most of the molecular structural parameters agree with those reported by Dou and Weiss.⁹ In the structure also obtained by us, the two non-equivalent C–Cl bonds have the same distances (1.701(6) and 1.702(6) Å) within the experimental errors. The distance (1.339(7) Å) of the localized $\text{C}(4)-\text{C}(5)$ bond is approximately equal to a typical $\text{C}=\text{C}$ double bond distance (1.337 Å), which differs from the corresponding distances (1.357–1.373 Å) in imidazole, 4-nitroimidazole, $(\text{CN})_2\text{Imd}$ and 2-amino-4,5-dicyanoimidazole.¹⁷ The imidazole ring of Cl_2Imd is planar with the mean deviation of 0.006 Å. The $\text{Cl}(5)$ atom is coplanar with the ring plane and the $\text{Cl}(4)$ deviates from the plane by 0.024 Å. The ORTEP view in Fig. 1(b) demonstrates that the largest amplitude of thermal ellipsoid is in the direction perpendicular to the molecular plane and to

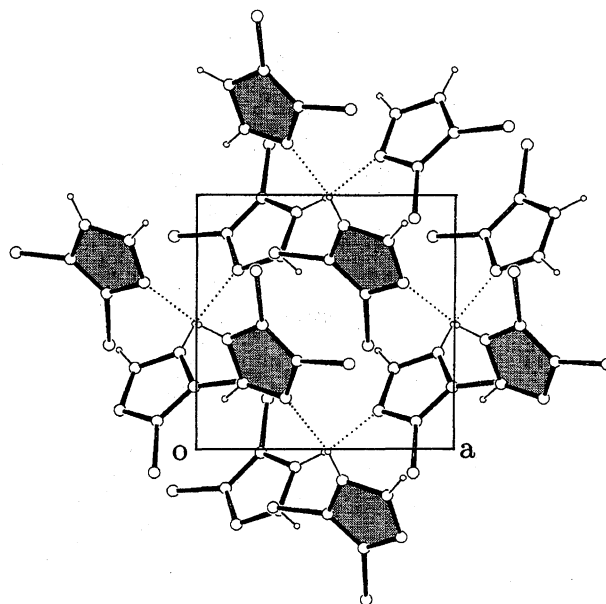


Fig. 2. Crystal structure of 4,5-dichloroimidazole projected along the c axis. One dimensional $\text{N}-\text{H}\cdots\text{N}$ hydrogen bonds are represented by dotted lines. Molecules near $z=0$ and $1/4$ (shaded molecules) are shown, while those near $1/2$ and $3/4$ are eliminated for clarifying the crystal structure.

the one-dimensional hydrogen-bonded chain.

The powder X-ray diffraction pattern at 4 K was almost identical with that at room temperature, indicating no phase transition in Cl_2Imd crystal down to 4 K. The lattice parameters at 4 K are $a=6.76(2)$ and $c=23.9(4)$ Å.

2. Structure and Spectroscopic Properties of $(\text{CN})_2\text{Imd}$. There exist two kinds of hydrogen bonds in $(\text{CN})_2\text{Imd}$, as shown by dotted (A) and broken lines (B) in Fig. 4. One of the ring nitrogen atoms is linked to the cyano nitrogen atoms of two neighboring molecules and the other ring nitrogen atom does not participate in the hydrogen bonding. Thus the hydrogen bond scheme is different from that in Cl_2Imd mentioned above. The hydrogen bond distances of $\text{N}\cdots\text{N}$ ($\text{N}\cdots\text{H}$) are 3.051(2) Å (2.22(2) Å) and 2.918(2) Å (2.25(3) Å) for A and B, respectively. The bond angles of $\text{N}-\text{H}\cdots\text{N}$ are 144(2)° for A and 126(2)° for B. Although two kinds of intermolecular hydrogen bonds were also found in 2-amino-4,5-dicyanoimidazole,¹⁷ the bond scheme is different from that of $(\text{CN})_2\text{Imd}$; the strong hydrogen bond (2.756(2) Å) is formed between the ring nitrogen atoms and the other weak hydrogen bond (3.127(2) Å and 3.195(3) Å) exists between the cyano and the amino nitrogen atoms.

The weak hydrogen bonds in $(\text{CN})_2\text{Imd}$ were confirmed by IR spectrum, as shown in Fig. 5(c). The $\text{N}-\text{H}$ stretching band is sharper and appears in a higher frequency region, 3260 cm^{-1} , than that in Cl_2Imd . The ^{15}N CP/MAS NMR spectrum gave sharp lines with the chemical shifts: $>\text{N}(1)-$, –210.5 ppm; $=\text{N}(3)-$, –118.0 ppm; $-\text{CN}(42)$ and $-\text{CN}(52)$, –109.2 ppm (the number-

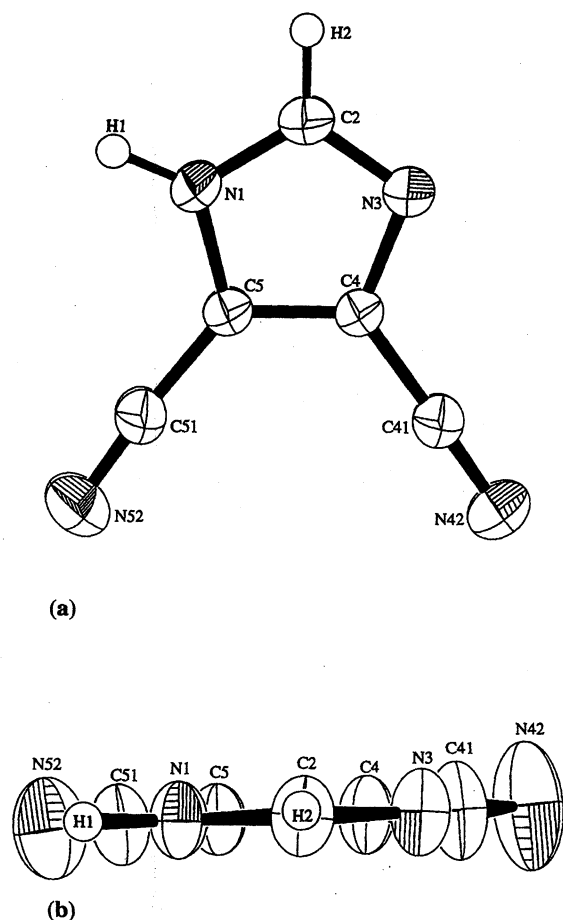


Fig. 3. ORTEP views of 4,5-dicyanoimidazole with a numbering scheme; viewed along a direction perpendicular to the plane of the ring (a) and parallel to one (b). Thermal ellipsoids are shown at 50% probability level.

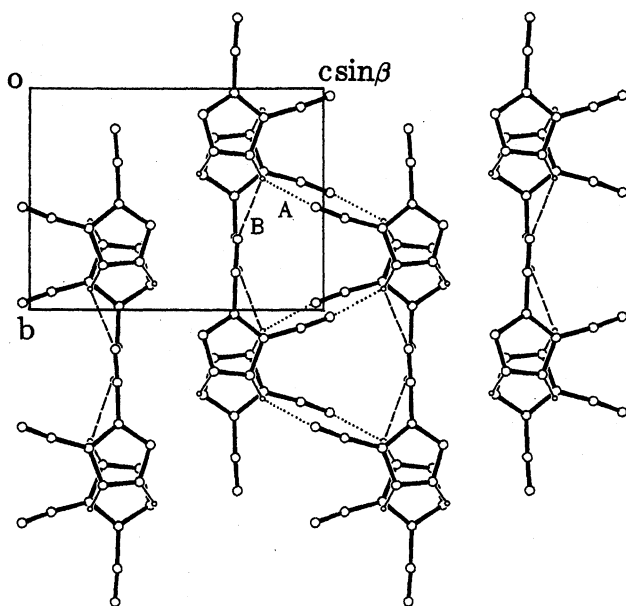


Fig. 4. Crystal structure of 4,5-dicyanoimidazole projected along the *a* axis.

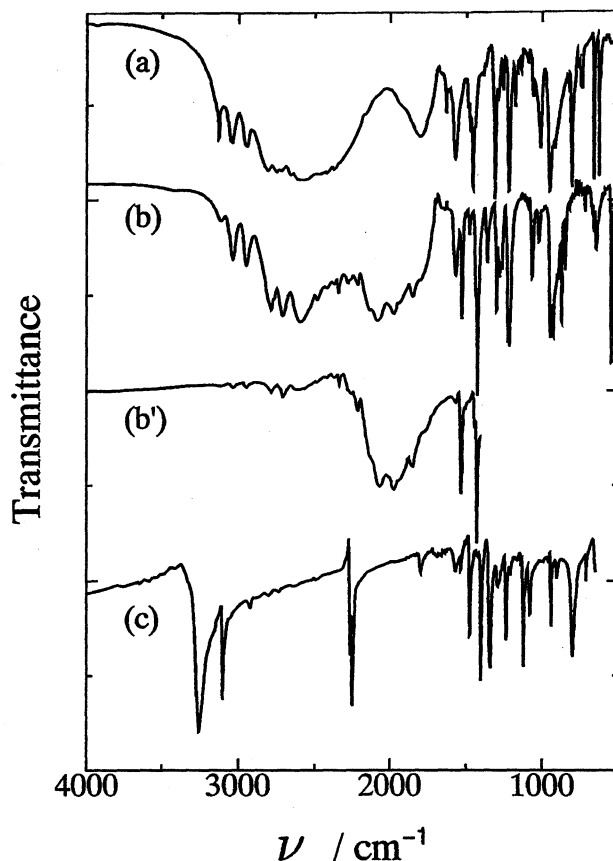


Fig. 5. Infrared spectra of (a) 4,5-dichloroimidazole, (b) partially deuterated 4,5-dichloroimidazole, (b') almost completely deuterated 4,5-dichloroimidazole, and (c) 4,5-dicyanoimidazole. Spectra (a), (b), and (c) were measured in KBr disks and (b') in Fluorinert (FC40) at room temperature. FC40 is transparent for IR above 1400 cm^{-1} .

ing of nitrogen atoms are given in Fig. 3). The observed values of chemical shifts of the ring nitrogen atoms may be compared with those (-219.2 and -119.1) of 1-methylimidazole in the dimethyl sulfoxide ($(\text{CH}_3)_2\text{SO}$) solution, which shows no tautomerism. Two ring nitrogens, $>\text{N}-$ and $=\text{N}-$, can be clearly distinguished, in contrast to the fact that imidazole in solution gives an averaged chemical shift, -169 ppm, due to the fast proton exchange between two nitrogens.¹⁸⁾

The C(4)–C(5) bond distance of $1.373(2)\text{ Å}$ is significantly longer than the corresponding values of Cl_2Imd and imidazole ($1.359(6)\text{ Å}$ at 123 K), but it can be compared with those ($1.373(4)$ and $1.371(4)\text{ Å}$) in 2-amino-4,5-dicyanoimidazole. It is obvious that the strong electron-withdrawing tendency of the cyano groups works in the crystal. The imidazole ring of $(\text{CN})_2\text{Imd}$ is planar with mean deviation of 0.001 Å and the cyano groups deviate from the plane between -0.045 and $+0.021\text{ Å}$. The ORTEP view in Fig. 3(b) indicates that the largest displacement of each thermal ellipsoid occurs in a direction perpendicular to the molecular plane, as in the case of Cl_2Imd . This is interesting from the viewpoint

of a dynamic perturbation on the hydrogen bonds in a chain.

The author (S.T.) is grateful for the financial support of the Ministry of Education, Science and Culture (Specially Promoted Research No. 06101004).

References

- 1) G. Will, *Nature (London)*, **198**, 575 (1963).
 - 2) G. Will, *Z. Kristallogr.*, **129**, 211 (1969).
 - 3) S. Martinez-Carrera, *Acta Crystallogr.*, **20**, 783 (1966).
 - 4) B. M. Craven, R. K. McMullan, J. D. Bell, and H. C. Freeman, *Acta Crystallogr., Sect. B*, **B33**, 2585 (1979).
 - 5) I. Ségalas, J. Poitras, and A. L. Beauchamp, *Acta Crystallogr., Sect. C*, **C48**, 295 (1992).
 - 6) H. L. De Bondt, E. Ragia, N. M. Blaton, O. M. Peeters, and C. J. De Ranter, *Acta Crystallogr., Sect. C*, **C49**, 693 (1993).
 - 7) P. Mirza, P. Agarmal, and R. C. Gupta, *Indian J. Pure Appl. Phys.*, **12**, 716 (1974).
 - 8) A. Kawada, A. R. McGhie, and M. M. Labes, *J. Chem. Phys.*, **52**, 3121 (1970).
 - 9) S. Dou and A. Weiss, *Z. Naturforsch., A*, **47A**, 177 (1992).
 - 10) S. Hayashi and K. Hayamizu, *Bull. Chem. Soc. Jpn.*, **64**, 688 (1991).
 - 11) G. M. Sheldrick, "SHELXS86. Program for the Solution of Crystal Structures," University of Göttingen, Germany (1985).
 - 12) F. Hai-Fu, "SAPI91. Structure Analysis Programs with Intelligent Control," Rigaku Corporation, Tokyo, Japan (1991).
 - 13) P. T. Beurskens, G. Admiraal, G. Beurskens, W. P. Bosman, S. Garcia-Granda, R. O. Gould, J. M. M. Smits, and C. Smykalla, "DIRDIF92. The DIRDIF Program System, Technical Report of the Crystallography Laboratory," University of Nijmegen, The Netherlands (1992).
 - 14) Molecular Structure Corporation, "teXsan. Crystal Structure Analysis Package," MSC, 3200 Research Forest Drive, The Woodlands, TX77381, USA (1985 & 1992).
 - 15) C. K. Johnson, "ORTEP II. Report ORNL-5138," Oak Ridge National Laboratory, Oak Ridge, Tennessee, USA (1976).
 - 16) E. Grech, Z. Malarski, and Sobczyk, *Spectrochim. Acta, Part A*, **48A**, 519 (1992).
 - 17) G. L. Hardgrove, Jr., and S. D. Jones, *Acta Crystallogr., Sect. C*, **C47**, 337 (1991).
 - 18) B. C. Chen, W. von Philipsborn, and K. Nagarajan, *Helv. Chim. Acta*, **66**, 1537 (1983).
-